Adaptive Linear and Extended KALMAN Filter applied to AMB with Collocated Position Measuring

Thomas Schuhmann, Wilfried Hofmann
Dept. Electrical Machines and Drives
Chemnitz University of Technology
Reichenhainer Str. 70, 09126 Chemnitz, Germany
thomas.schuhmann@etit.tu-chemnitz.de
wilfried.hofmann@e-technik.tu-chemnitz.de

Ralf Werner
Dept. Electrical Drives
Mittweida University of Applied Sciences
Technikumplatz 17, 09648 Mittweida, Germany
rwerner@htwm.de

***Abstract*— In the majority of cases, magnetically levitated rotors are equipped with externally mounted position sensors, i.e. a dislocation between bearing and sensor plane occurs. The disparity between actual and measured rotor position can cause system instability due to natural oscillations of the shaft. This paper proposes a method for avoiding this problem by integrating capacitive position sensors straight into the stator laminations of a radial magnetic bearing. The stronger sensor noise originating from the proximity between bearing coils and sensors can be reduced effectively by means of a stochastical state estimator. Different types of KALMAN filters used for these purposes, both linear and extended ones, are presented in this paper. It is shown how unknown bearing parameters can be estimated by means of the filter. Concluding, a LQG controller (optimal controller combined with optimal state estimator) is presented and compared to an optimally parametrised PID controller. All methods proposed in this paper are approved by measurements.**

***Index Terms*— Magnetic Levitation, LQG Control, Kalman Filtering, Capacitive Sensors.**

I. INTRODUCTION

The system inherent instability of magnetically levitated shafts or self-bearing motors requires a fast and accurate measurement of the actual rotor position. A variety of sensing technologies has been developed and used for these purposes [1]. These technologies usually have one attribute in common – the external application of the sensors by means of an additional measuring trace. However, it is a well known fact that natural oscillation modes of the rotor in combination with the spatial dislocation between measuring plane and bearing laminations can cause stability problems [2]. In worst case, the natural modes are even excited by the controller due to a nodal point located between laminated core and measuring trace. This problem can be solved by means of mechanical modifications, additional sensors or sophisticated control.

Another approach, which is little applied up to now, is to avoid dislocation by obtaining the position information in-plane with the bearing laminations. For this reason, a radial active magnetic bearing ($F_r = 2400\,\mathrm{N}$) was fitted out with capacitive position sensors which are fully integrated into the pole gap of the stator laminations (Fig. 1).

This work is supported by Deutsche Forschungsgemeinschaft (German Research Foundation).

The sensors consist of simple copper-cladded material. To achieve better linearity, two opposite sensors are used for each bearing axis, whereas the difference between both capacitances is evaluated in a bridge circuit [3]. The bridge is driven by a high-frequent, constant amplitude carrier voltage. For demodulating the amplitude-modulated signal, an in-phase rectifier with an narrow-band bandpass is used. More detailed information referring to the measurement system can be found in [4].

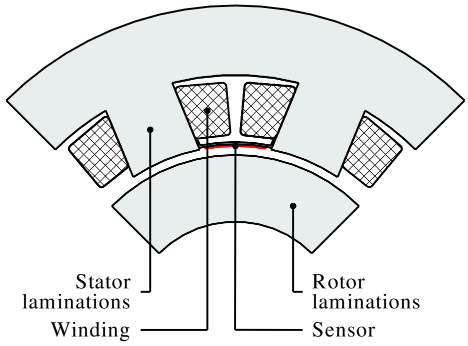

Fig. 1. Section of radial magnetic bearing with integrated capacitive position sensor.

Practical investigations have been made by dint of an unilaterally magnetically levitated test rotor (mass 25 kg, length 910 mm). Integrated capacitive sensors are installed on the test rig as well as conventionally eddy current sensors (with an externally mounted measuring trace made of aluminium). The test rotor exhibits difficult dynamic behaviour with regard to the lower oscillation modes. In particular, the third natural oscillation mode possesses an nodal point which is located quite close to the rotor laminations of the bearing, as can be seen in Fig. 2. It is obvious that this oscillation mode ($i = 3$) is not controllable, if the eddy current sensors are used. Because of the positive position feedback, the system will start oscillating with the corresponding natural frequency (Fig. 2, upper diagram). If the controller gains are chosen too high, instability is unavoidable. By using the integrated capacitive sensors instead, the dynamic behaviour of the system can be improved significantly, because of the absent excitation of a

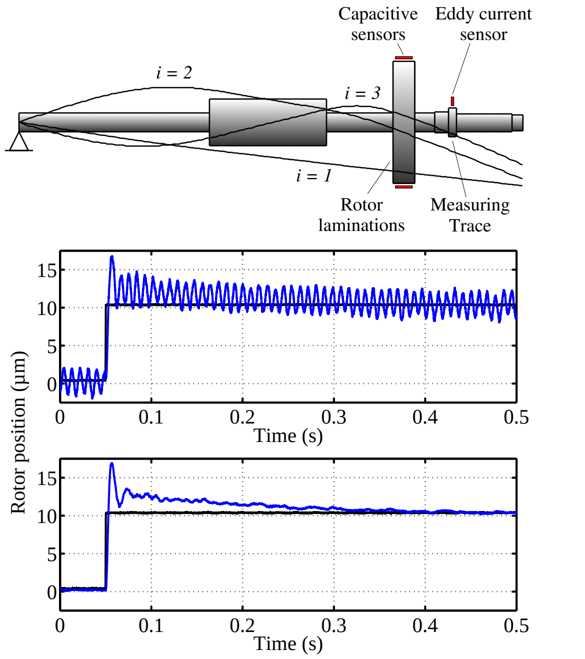

Fig. 2. Influence of position sensor arrangement on dynamic behaviour of magnetically levitated rotor (Top – sketch of test rotor with natural oscillation modes $i = 1 \dots 3$, Middle – step response with external eddy current sensors, Bottom – step response with integrated capacitive sensors).

low-order natural oscillation. The lower diagram in Fig. 2 proves this proposition. This heightened system stability enables the user to increase the proportional and derivative gains of the position controller which yields better stiffness and damping of the bearing. On the test rig, enlarging the controller gains about more than 75 % has been possible. – Another advantage of the capacitive measuring system, which is quite simple to manufacture, is the possibility to reduce axial installation length of the radial bearing about 20 to 30 % because of the absent necessity for incorporating an additional measuring trace.

II. Measurement Preprocessing with Linear Kalman Filter

The advantage of gaining position information of the magnetically levitated rotor in-plane with the bearing laminations entails the disadvantage of stronger sensor noise (caused by the proximity of the sensors to the bearing windings) and thus reduced positioning control accuracy. One possible solution is to implement a stochastical state estimator or Kalman filter to reduce the effective sensor noise. The filter contains a model of the considered system. Just like an observer, it predicts system states and outputs on the basis of this internal model. The estimated outputs are compared with the real measured, noisy output signals. System noise (caused by modelling inaccuracies) and measurement noise are taken into account explicitly [6]. The system has to be modelled in state space form

$$\left.\begin{array}{rcl} \boldsymbol{x}_{k+1} & = & \boldsymbol{A}_k \boldsymbol{x}_k + \boldsymbol{B}_k \boldsymbol{u}_k + \boldsymbol{\xi}_k \\ \boldsymbol{y}_k & = & \boldsymbol{C}_k \boldsymbol{x}_k + \boldsymbol{\eta}_k \end{array}\right\} \qquad (1)$$

with $\boldsymbol{\xi}_k$ process noise and $\boldsymbol{\eta}_k$ measurement noise, both sequences of zero-mean Gaussian white noise. The time-discrete filter algorithm can be outlined as [7]

$$\left.\begin{array}{l} \textit{Prediction step:} \\ \hat{\boldsymbol{x}}_{k|k-1} = \boldsymbol{A}_{k-1}\hat{\boldsymbol{x}}_{k-1|k-1} + \boldsymbol{B}_{k-1}\boldsymbol{u}_{k-1} \\ \boldsymbol{P}_{k|k-1} = \boldsymbol{A}_{k-1}\boldsymbol{P}_{k-1|k-1}\boldsymbol{A}_{k-1}^T + \boldsymbol{Q}_{k-1} \\ \\ \textit{Correction step:} \\ \boldsymbol{K}_k = \boldsymbol{P}_{k|k-1}\boldsymbol{C}_k^T\left(\boldsymbol{C}_k\boldsymbol{P}_{k|k-1}\boldsymbol{C}_k^T + \boldsymbol{R}_k\right)^{-1} \\ \hat{\boldsymbol{x}}_{k|k} = \hat{\boldsymbol{x}}_{k|k-1} + \boldsymbol{K}_k\left(\boldsymbol{y}_k - \boldsymbol{C}_k\hat{\boldsymbol{x}}_{k|k-1}\right) \\ \boldsymbol{P}_{k|k} = \left(\boldsymbol{I} - \boldsymbol{K}_k\boldsymbol{C}_k\right)\boldsymbol{P}_{k|k-1} \end{array}\right\} \qquad (2)$$

with $\hat{\boldsymbol{x}}$ optimal estimation of state vector, $\boldsymbol{u}$ deterministic control input vector, $\boldsymbol{y}$ measurement vector, $\{\boldsymbol{A}\ \boldsymbol{B}\ \boldsymbol{C}\}$ discrete time system model matrices, $\boldsymbol{P}$ covariance matrix of estimation error, $\boldsymbol{Q}$ covariance matrix of system (i.e.) process noise, $\boldsymbol{R}$ covariance matrix of measurement noise and $\boldsymbol{K}$ an optimal gain matrix for correcting the predicted system states with the new measurement data. The notation $(\mu|\nu)$ denotes an estimation at time step μ with measurement information from time step ν.

For computation time reasons, it is recommendable to reduce the length of the state vector and therewith the dimensions of most matrices in (2) as far as possible. Hence a decentralised filter structure is preferable (i.e. each bearing axis is observed by means of one independent Kalman filter). To use the linear filter algorithm, a linear system model is required. The force f_m acting on the test rotor is described by

$$f_m = m\frac{dv}{dt} = m\frac{d^2x}{dt^2} = k_x \cdot x + k_i \cdot i \qquad (3)$$

with k_x force-position-factor, k_i force-current-factor, m equivalent rotor mass. Radial rotor velocity v is connected to rotor position x via $v = \frac{dx}{dt}$. The dynamic behaviour of the pulse amplifier and the electrical part of the bearing is subsumed to one first-order lag element

$$T_a\frac{di}{dt} + i = K_a i_{ref} \qquad (4)$$

with T_a equivalent time constant of electrical plant, K_a amplifier gain and i control current. This elementary approach provides a system model with three state variables $\boldsymbol{x}^T = (x\ v\ i)$ and one control input $\boldsymbol{u} = i_{ref}$. The experimental test rig under investigation allows measurement of position and control current, thus the measurement vector is $\boldsymbol{y}^T = (K_{mx}\,x \quad K_{mi}\,i)$. A linear filter using this approach has been implemented on a TMS320C240 DSP (sampling time 50 µs). The improvement, which has been achieved by using the optimally estimated rotor position signal instead of the measured signal as control variable for the position control loop, is depicted in Fig. 3. The rotor oscillation amplitude around the reference position could be reduced about approx. 80 % in standstill, which enabled us to heighten the PID controller gains about 75 %. – Estimating unknown system parameters $p(t)$ by means of the linear KALMAN filter is possible, if the dependency of these parameters is a linear one. Then the state vector can be augmented by p, and the modelling can be made by $\frac{dp}{dt} = 0 + \xi_p$ if no deterministic law for the change of p can be found. Thus, any changes of the unknown parameter are modelled only by means of the process noise $\boldsymbol{\xi}$. More detailed information concerning the system modelling and the choice of the filter noise variance matrices has been given in [4] and must be omitted here.

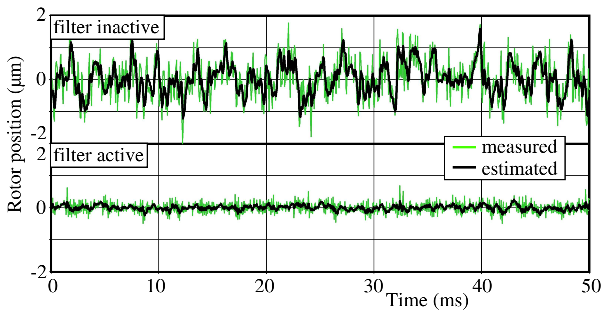

Fig. 3. Improvement of position control accuracy by means of KALMAN filter at standstill (Top – measured position as control variable, Bottom – estimated position as control variable).

III. State and Parameter Estimation with Extended Kalman Filter

One of the most important benefits of the KALMAN filter is its ability for estimating unknown system parameters, even if a change of these parameters cannot be described in any deterministic way. For this purpose, the state vector $\boldsymbol{x}$ has to be augmented by the parameters which are of interest. Presumably, most of these parameters are coupled with other state variables in a multiplicative or another non-linear way, and therewith a linear state space model in the manner of (1) is not assignable any longer. The same problem appears if the system itself is described by non-linear equations (as it is generally the case with any magnetic bearing before carrying out a linearisation). In such cases, the linear KALMAN filter algorithm (2) is not applicable, and the extended KALMAN filter has to be utilised [6][7]. The system is described by two non-linear vector-valued functions

$$\boldsymbol{x}_{k+1} = \boldsymbol{f}_k(\boldsymbol{x}_k, \boldsymbol{u}_k) + \boldsymbol{\xi}_k \qquad \boldsymbol{y}_k = \boldsymbol{g}_k(\boldsymbol{x}_k) + \boldsymbol{\eta}_k. \quad (5)$$

Any changes of unknown parameters are modelled by $\boldsymbol{\xi}_k$. The filter algorithm can be outlined as

$$\left.\begin{array}{l} \textit{Prediction step:} \\ \hat{\boldsymbol{x}}_{k|k-1} = \boldsymbol{f}_{k-1}\left(\hat{\boldsymbol{x}}_{k-1|k-1}, \boldsymbol{u}_{k-1}\right) \\ \boldsymbol{P}_{k|k-1} = \boldsymbol{\Phi}_{k-1}\boldsymbol{P}_{k-1|k-1}\boldsymbol{\Phi}_{k-1}^T + \boldsymbol{Q}_{k-1} \\ \\ \textit{Correction step:} \\ \boldsymbol{K}_k = \boldsymbol{P}_{k|k-1}\boldsymbol{\Gamma}_k^T\left(\boldsymbol{\Gamma}_k\boldsymbol{P}_{k|k-1}\boldsymbol{\Gamma}_k^T + \boldsymbol{R}_k\right)^{-1} \\ \hat{\boldsymbol{x}}_{k|k} = \hat{\boldsymbol{x}}_{k|k-1} + \boldsymbol{K}_k\left(\boldsymbol{y}_k - \boldsymbol{g}_k\left(\hat{\boldsymbol{x}}_{k|k-1}\right)\right) \\ \boldsymbol{P}_{k|k} = \left(\boldsymbol{I} - \boldsymbol{K}_k\boldsymbol{\Gamma}_k\right)\boldsymbol{P}_{k|k-1} \end{array}\right\} \quad (6)$$

with the JACOBI matrices

$$\left.\begin{array}{l} \boldsymbol{\Phi}_{k-1} = \frac{\partial \boldsymbol{f}_{k-1}\left(\hat{\boldsymbol{x}}_{k-1|k-1}, \boldsymbol{u}_{k-1}\right)}{\partial \boldsymbol{x}_{k-1}} \\ \boldsymbol{\Gamma}_k = \frac{\partial \boldsymbol{g}_k\left(\hat{\boldsymbol{x}}_{k|k-1}\right)}{\partial \boldsymbol{x}_k} \end{array}\right\} \quad (7)$$

which realise a linearisation of the system round the actual estimated state trajectory at each time step. Basically, there exist two approaches for employing the extended KALMAN filter in combination with magnetic bearing applications:

- Linearising the system model and augmenting the state vector by non-linear coupled parameters or
- applying a non-linear system model right from the start.

Both variants have been investigated and shall be delineated subsequently.

A. Linearised Bearing Model

If the simple linearised model from section II for one bearing axis is used and the state vector is augmented by the parameters force-current-factor $k_i(t)$ and force-position-factor $k_x(t)$

$$\boldsymbol{x}^T(t) = [x(t)\ v(t)\ i(t)\ k_i(t)\ k_x(t)], \quad (8)$$

the resulting non-linear vector-valued functions in equations (5) can be written as (in continuous time)

$$\left.\begin{array}{l} \boldsymbol{f}(\boldsymbol{x}, \boldsymbol{u}) = \begin{pmatrix} v \\ \frac{k_x}{m}x + \frac{k_i}{m}i \\ \frac{K_a}{T_a}i_{ref} - \frac{1}{T_a}i \\ 0 \\ 0 \end{pmatrix} \\ \\ \boldsymbol{g}(\boldsymbol{x}) = \begin{pmatrix} K_{mx}\ x \\ K_{mi}\ i \end{pmatrix}. \end{array}\right\} \quad (9)$$

The estimation of the states $x(t)$, $v(t)$ and $i(t)$ at the actual time step is based on the parameters $k_i(t-T)$ and $k_x(t-T)$ which have been estimated at the previous time step (T sampling time). The algorithm has been implemented on a TMS320C240 DSP (dSPACE® environment) with a sampling time of 50 µs. Experiments on the test rig have shown that both noise reduction and parameter estimation work well, although it came out that a proper estimation of k_i and k_x does require an adequate system excitement. This has been realised by means of an additional PRBS (Pseudo Random Binary Sequence) signal which was superimposed to the reference position signal [4]. This necessity for exerting influence on the system seems to be the main drawback of this modelling method.

B. Non-Linear Bearing Model

A quite different approach is describing the bearing by means of a non-linear model. This is an obvious procedure since the bearing is a non-linear system by nature, and any previously implemented linearisation (as in the both cases described in the previously sections) will implicate errors when estimating states and parameters. The essential quantity in the system is the magnetic force f_m acting on the levitated rotor. The test bearing is a eight pole, heteropolar radial bearing. Each magnet consists of two adjacent poles which carry both a winding for premagnetising current i_{prem} and one winding for control current i (differential principle). The magnetic force generated by each magnet can be expressed by [8]

$$f_m(x,i) = c_f \left[\frac{(i_0+i)^2}{(\delta_0 - x\cos\alpha)^2} - \frac{(i_0-i)^2}{(\delta_0 + x\cos\alpha)^2} \right] \quad (10)$$

with c_f a bearing constant containing design specific parameters (pole area, number of turns...), i_0 the related premagnetising current (i_{prem} times the ratio of premagnetising and control winding turns), i control current, x rotor displacement with reference to the centre position, δ_0 the nominal air gap and α the pole angle between centre of pole area and centre of magnet (all relevant parameters can be found in the appendix). The state variable velocity v is determined by NEWTONs second law

$$\frac{dv}{dt} = \frac{1}{m}(f_m + f_z) \quad (11)$$

with an additional disturbance force f_z which is a parameter to be estimated. Further state variables are position x and control current i (cf. section II). The delay which is caused by the measurement system has been taken into account by augmenting the state vector with an additional, delayed rotor position x_d. The dynamic behaviour of the measurement system has been modelled as a first order lag element with the time constant T_{mx}:

$$T_{mx}\frac{dx_d}{dt} + x_d = x. \quad (12)$$

The basic idea behind this is to compare the real measured value with a delayed value of the estimated position and therewith to compensate the delay caused by the measuring system. For control purposes, of course the undelayed estimation of position is to be used. At last, the new state vector consists of five elements

$$\boldsymbol{x}^T(t) = [x(t)\ v(t)\ i(t)\ x_d(t)\ f_z(t)]\,. \quad (13)$$

The non-linear continuous-time state and measurement equations can now be formulated as

$$\left.\begin{aligned} \boldsymbol{f}(\boldsymbol{x},\boldsymbol{u}) &= \begin{pmatrix} v \\ \frac{1}{m}c_f\left[\frac{(i_0+i)^2}{(\delta_0-x\cos\alpha)^2} - \frac{(i_0-i)^2}{(\delta_0+x\cos\alpha)^2}\right] + \frac{1}{m}f_z \\ \frac{K_a}{T_a}i_{ref} - \frac{1}{T_a}i \\ \frac{1}{T_{mx}}x - \frac{1}{T_{mx}}x_d \\ 0 \end{pmatrix} \\ \boldsymbol{g}(\boldsymbol{x}) &= \begin{pmatrix} K_{mx}\ x_d \\ K_{mi}\ i \end{pmatrix}. \end{aligned}\right\} \quad (14)$$

Again, the unknown disturbance force f_z is modelled only by means of process noise. To implement the algorithm (6) on a signal processor, the discrete JACOBI matrixes $\boldsymbol{\Phi}$ and $\boldsymbol{\Gamma}$ are required. These can be calculated by computing the continuous-time matrices $\boldsymbol{F} = \frac{\partial \boldsymbol{f}(\boldsymbol{x},\boldsymbol{u})}{\partial \boldsymbol{x}}$ and $\boldsymbol{G} = \frac{\partial \boldsymbol{g}(\boldsymbol{x})}{\partial \boldsymbol{x}}$. Subsequently, the matrix $\boldsymbol{\Phi}$ has to be calculated by discretising $\boldsymbol{F}$ by means of a series expansion of the matrix exponential function $\boldsymbol{\Phi} = \mathrm{e}^{\boldsymbol{F}T}$ (T sampling time). This expansion has been cancelled after the third term so that

$$\boldsymbol{\Phi}(T) = \boldsymbol{I} + \boldsymbol{F}T + \frac{1}{2}\boldsymbol{F}^2T^2 \quad (15)$$

($\boldsymbol{I}$ identity matrix). $\boldsymbol{\Gamma}$ is identical to $\boldsymbol{G}$ if the input vector is piecewise constant. The prediction of the state vector (first equation in (6)) is executed by using a fourth-order RUNGE-KUTTA integration method. After implementing the filter on a dSPACE® environment, the noise variance matrices have been set to

$$\boldsymbol{R} = \mathrm{diag}\left\{7.1\cdot 10^{-4}\,\mathrm{V}^2 \quad 1.4\cdot 10^{-1}\,\mathrm{V}^2\right\} \quad (16)$$

$$\boldsymbol{Q} = \mathrm{diag}\left\{0\,\mathrm{m}^2 \quad 2.6\cdot 10^{-10}\,\frac{\mathrm{m}^2}{\mathrm{s}^2} \quad 4.3\cdot 10^{-1}\,\mathrm{A}^2 \quad 0\,\mathrm{m}^2 \quad 1\,\mathrm{N}^2\right\}. \quad (17)$$

By using the estimated rotor position x as control variable, the measurement noise caused oscillations have been reduced about approx. 80 %. The second main goal when implementing this non-linear filter has been estimation of unknown system parameters. Fig. 4 illustrates the operation of estimating a unknown step-shaped disturbance force acting on the rotor (the dynamic behaviour of the filter has been varied by tuning the element q_{55} of $\boldsymbol{Q}$). This ability of estimating highly dynamic disturbances can be used for implementing a disturbance feedforward.

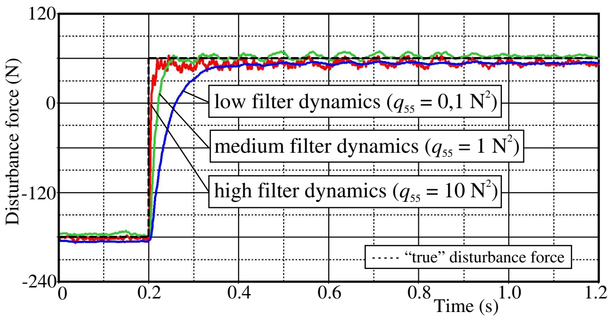

Fig. 4. Estimation of step shaped disturbance force f_z (variable estimator dynamics).

As already mentioned, the extended KALMAN filter algorithm is based on linearising the system model *around the actual operating point* by calculation of $\boldsymbol{\Phi}_k$. This allows to state a linear system description in any arbitrarily chosen system state. The linearising factors (which are k_i and k_x if the elementary model of section II is used) must be detectable in $\boldsymbol{\Phi}_k$. It can bee shown that the two parameters can be calculated out of particular elements of $\boldsymbol{\Phi}_k$ via

$$k_{x,k} = \frac{2m}{T^2}(\Phi_{11,k} - 1) \quad \text{and} \quad k_{i,k} = \frac{2m}{T^2}\Phi_{13,k}. \quad (18)$$

Fig. 5 shows the dynamic estimation of force-position- and force-current-factor in dependency of the actual rotor position (static load $f_z = 200\,\mathrm{N}$ applied). Detecting such fast time-variant changes of system parameters is quite useful if an adaptive controller shall be utilised. It should be emphasised that no additional system excitement is necessary in this case, contrary to the filter with a linear system model which has been described in section III-A.

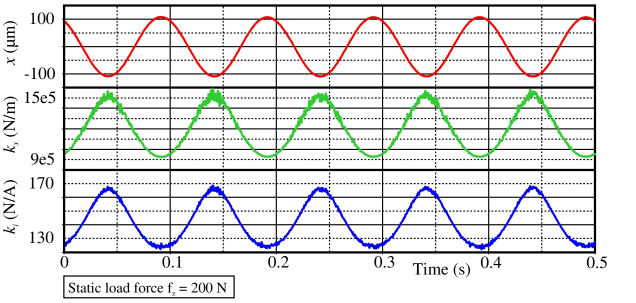

Fig. 5. Estimation of time varying system parameters (Top – actual rotor position, Middle – estimation of force-position-factor k_x, Bottom – estimation of force-current-factor k_i).

IV. LQG Control of Active Magnetic Bearing

In addition to noise reduction and estimation of unknown parameters, integrating a KALMAN filter yields another essential advantage. The availability of all system states offers the possibility to implement a full-order state feedback controller for the magnetic bearing. Combining an optimal state estimator with an optimal state space controller leads to a regulator which is known as LQG controller (**L**inear system model, **Q**uadratic optimising criterion, **G**aussian disturbances) [5]. The regulator is able to transfer the system states $\boldsymbol{x}$ from any arbitrarily chosen initial condition $\boldsymbol{x}_0$ to the aspired final condition $\boldsymbol{x}_k = \boldsymbol{0}$. The structure of the controlled system can be seen in Fig. 6. Due to the fact that external disturbance forces would cause steady positioning errors, and since step-shaped changes of the reference position are to be followed, the LQG structure has been superimposed by an integral controller which is able to correct potentially occurring control deviations.

The optimal state feedback vector $\boldsymbol{K}$ can be calculated by examining the optimality criterion

$$J\left(\boldsymbol{x}_0, \boldsymbol{u}\right) = \sum_{k=0}^{\infty} \left(\boldsymbol{x}_k^T \boldsymbol{Q}_J \boldsymbol{x}_k + \boldsymbol{u}_k^T \boldsymbol{R}_J \boldsymbol{u}_k\right). \quad (19)$$

The optimising problem $\min_{\boldsymbol{K}} J\left(\boldsymbol{x}_0, \boldsymbol{u}\right)$ leads to a matrix-valued RICCATI equation

$$\boldsymbol{P}_J = \boldsymbol{Q}_J + \boldsymbol{A}^T \boldsymbol{P}_J \boldsymbol{A} - \\ -\boldsymbol{A}^T \boldsymbol{P}_J \boldsymbol{B} \left(\boldsymbol{R}_J + \boldsymbol{B}^T \boldsymbol{P}_J \boldsymbol{B}\right)^{-1} \boldsymbol{B}^T \boldsymbol{P}_J \boldsymbol{A} \quad (20)$$

whose solution $\boldsymbol{P}_J$ allows computing the controller gains according to

$$\boldsymbol{K} = \left(\boldsymbol{R}_J + \boldsymbol{B}^T \boldsymbol{P}_J \boldsymbol{B}\right)^{-1} \boldsymbol{B}^T \boldsymbol{P}_J \boldsymbol{A}. \quad (21)$$

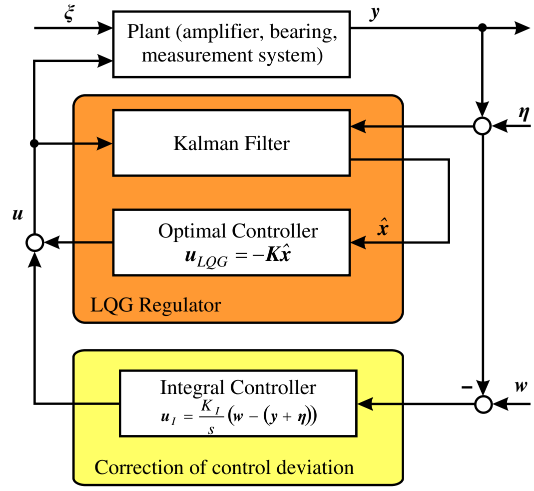

Fig. 6. LQG controlled system ($\boldsymbol{\xi}$ process and $\boldsymbol{\eta}$ measurement noise).

The matrices $\boldsymbol{Q}_J$ and $\boldsymbol{R}_J$ in (19) are weighting any deviation of the state variables or the control variables, respectively. The strategy for choosing the elements of these matrices has already been described in [4]. A decentralized controller for the three integral state variables $\boldsymbol{x}^T = (x \ v \ i)$ has been implemented on a TMS320C240 DSP (dSPACE® environment). The controller output signal $\boldsymbol{u} = i_{ref}$ acts as reference input for the subordinate (analog regulated) current control loop. The optimal controller gains have been found to

$$\boldsymbol{K} = \left(9.979 \cdot 10^3 \quad 29.686 \quad 0.073\right). \quad (22)$$

The gain for the superimposed integrative controller has been chosen to $K_I = 1.03 \cdot 10^6\,\mathrm{s}^{-1}$. If we assume the nominal bearing parameters (which can be found in the appendix) to be true, we receive an pole allocation of the LQG controlled system as can be seen in Fig. 7. For comparison, the poles of an appropriate state estimator are depicted (in this case a simple fourth order linear KALMAN filter after reaching the steady state). The dominant pole pair of the state estimator shows real parts which are more than five times the real parts of the dominant poles of the controlled system. This offers an adequate transient response of the observer structure.

Experimental investigations have been executed on the test rig for permitting an objective comparison between a conventional PID controller and the LQG regulator. Fig. 8 shows the step response of the rotor position and the appendant control current. The optimal PID controller parameters have been computed by means of root locus method ($K = 0.65, T_I = 50\,\mathrm{ms}, T_D = 3\,\mathrm{ms}$). Though the PID controlled rotor reacts faster on a change of the reference value, its transient time is very much bigger than the transient time of the LQG controlled system. Furthermore, the state space controlled rotor shows no overshoot at all. Another (and by far more important) advancement is the significantly reduced amplitude of the control current, which allows to save a large amount of control energy when performing such dynamic processes.

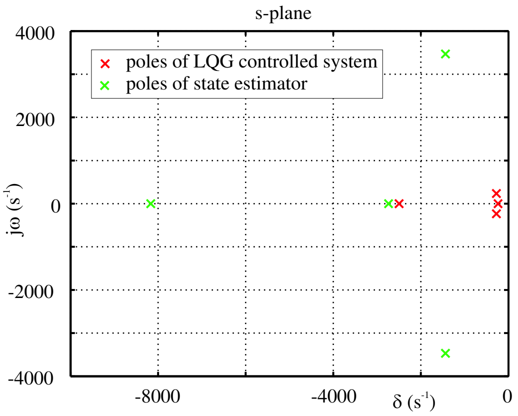

Fig. 7. Poles of the LQG controlled system (assuming the nominal parameter values to be true) compared to the poles of an appropriate KALMAN filter (after reaching steady state).

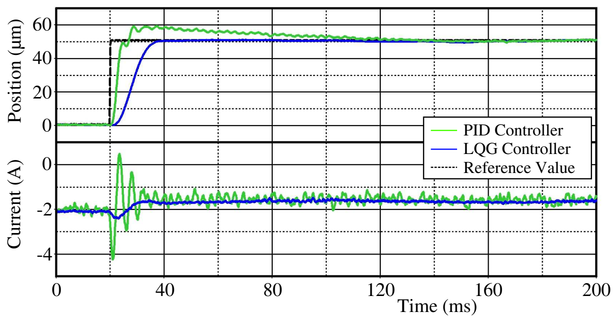

Fig. 8. Tracking behaviour of optimal PID and LQG regulator (reference value step $\Delta x = 50\,\mu\text{m}$).

The graphs in Fig. 9 illustrate the control behaviour of the magnetically levitated rotor in case of a step-shaped acting disturbance force ($\Delta f_z = 400\,\text{N}$). If we define the dynamic stiffness of the bearing $s_{dyn} = \frac{\Delta f_z}{\Delta x}$ with Δx the maximal rotor deviation from reference value, we get a stiffness of the LQG controlled system $s_{dyn,LQG} = 6.7\,\text{N}/\mu\text{m}$ which is almost two times the stiffness of the PID controlled system $s_{dyn,PID} = 3.6\,\text{N}/\mu\text{m}$.

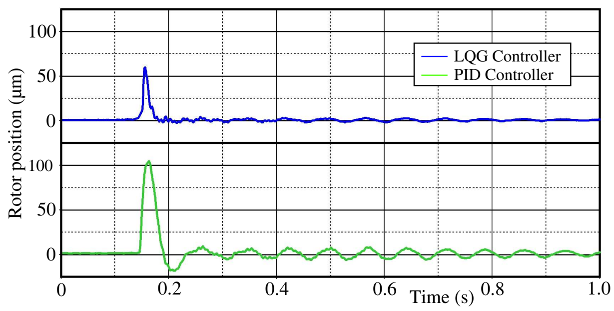

Fig. 9. Dynamic stiffness of optimal PID and LQG regulator (step-shaped disturbance force $\Delta f_z = 400\,\text{N}$).

V. CONCLUSION

The structural problems caused by spatial dislocation between radial magnetic bearings and position sensors can be overcome by integrating capacitive sensors into the stator laminations of the bearing. It has been shown in this paper that the stronger sensor noise can be reduced significantly by implementing linear or extended KALMAN filters. Next to noise reduction, these filters are able to estimate unknown system parameters (e.g. disturbance forces, force-current- and force-position-factors). In terms of estimation dynamics and necessary system excitement, the extended filter with non-linear system model has shaped up as the best alternative. – When implementing a stochastical state estimator, the availability of all system states suggests to use an full-order optimal state space controller. Such an LQG controller has been implemented on the test rig. It has been shown that this regulator is superior to conventional optimally parametrised PID controllers in terms of control behaviour and saving of control energy.

APPENDIX

TEST RIG PARAMETERS

Parameter	**Value**
Mass of test rotor	25 kg
Length of test rotor	910 mm
Rotor laminations diameter	272 mm
Rated bearing force (one axis) F_r	2400 N
Rated air gap δ	0.3 . . . 0.7 mm
Position measurement gain K_{mx}	20 mV/µm
Current measurement gain K_{mi}	0.2 V/A
Rated force-current-factor k_i	128.6 N/A
Rated force-position-factor k_x	800310 N/m
Equivalent rotor mass m	21.5 kg
Pulse amplifier gain K_a	5 A/V
Pulse amplifier equivalent time constant T_a	400 µs
Sampling time of DSP T (all algorithms)	50 µs
Force factor c_f	2.1935e-6 $\text{N}\cdot\text{m}^2/\text{A}^2$
Pole angle α	π/8

REFERENCES

[1] Boehm, J.; Gerber, R.; Kiley, N. R. C.: *Sensors for Magnetic Bearings.* IEEE Transactions on Magnetics, Vol. 29 (1993), No. 6, pp. 2962 - 2964.
[2] Schweitzer, G.; Bleuler, H.; Traxler, A.: *Active Magnetic Bearings. Basics, Properties and Applications of Active Magnetic Bearings.* Verlag der Fachvereine (vdf), ETH Zurich, Zurich, Switzerland, 1994.
[3] Baxter, L. K.: *Capacitive Sensors.* IEEE Press, Piscataway, 1997.
[4] Schuhmann, T.; Hofmann, W.; Werner, R.: *Sensor Integration and State Estimation on Magnetically Levitated Rotors.* In: Proceedings SPEEDAM 2006, pp. S11-11 – S11-16.
[5] Soederstroem, T.: *Discrete-time Stochastic Systems.* Springer, London, 2002.
[6] Brown, R. G.; Hwang, P. Y. C.: *Introduction to Random Signals and Applied Kalman Filtering.* Wiley, New York, 1997.
[7] Chui, C. K.; Chen, G.: *Kalman Filtering with Real-Time Applications.* Springer, Berlin, 1999.
[8] Hofmeyer, D.: *Kennfeldbasierte Schaltregelung fuer ein aktives Magnetlager.* VDI Verlag, Duesseldorf, 2000 (Fortschrittsberichte VDI Reihe 21 Nr. 296).